

Cite this: DOI: 10.1039/c1ee02181h

www.rsc.org/ees

PAPER

Charge transfer excitons in low band gap polymer based solar cells and the role of processing additives†

Markus C. Scharber,^{*a} Christoph Lungenschmied,^a Hans-Joachim Egelhaaf,^{ab} Gebhard Matt,^c Mateusz Bednorz,^c Thomas Fromherz,^c Jia Gao,^d Dorota Jarzab^d and Maria A. Loi^{*d}

Received 20th July 2011, Accepted 29th September 2011

DOI: 10.1039/c1ee02181h

Organic semiconductor blends yielding efficient charge generation and transport are key components for the development of high performance organic bulk-heterojunction solar cells. In this paper the effect of the processing additive octane-dithiol on the charge transfer emission in poly[2,6-(4,4-bis-(2-ethylhexyl)-4*H*-cyclopenta[2,1-*b*;3,4-*b'*]-dithiophene)-*alt*-4,7-(2,1,3-benzothiadiazole)] (PCPDTBT) and [6,6]-phenyl-C₆₁-butyric acid methyl ester (PCBM) is investigated. Despite the fact that blends processed with and without additive show a ground state charge transfer optical absorption only the blend processed without additive shows a corresponding charge transfer emission. The presented experimental data show that the nano-morphology of the bulk-heterojunction blends plays an important role for the formation of emissive charge transfer excitons, and that it is a loss channel in the studied solar cells.

Introduction

Bulk heterojunction solar cells have attracted considerable attention over the past few years due to their potential for being one of the first ultra-low-cost photovoltaic (PV) technologies. The possibility of manufacturing PV modules in a roll-to-roll

process in combination with low-cost active materials could lead to a watt-peak price below 0.5 US\$ in the near future.¹

Efficiencies of bulk heterojunction (BHJ) solar cells larger than 8% have been reported and certified by the National Renewable Energy Laboratory (NREL).² Theoretical and experimental studies suggest that power conversion efficiencies in the range of 10–12% can be achieved with single junction devices, which is significantly lower than the maximum efficiency predicted by the Shockley–Queisser-limit.^{3,4}

Several different factors limiting the performance of BHJ solar cells have been identified, including the nano-morphology⁵ of the photoactive layer, losses due to charge carrier recombination,⁶ inefficient charge transport⁷ and the non-optimized offset between the donor and the acceptor level.^{3,8}

Recently, a weak optical band assigned to a charge transfer transition has been observed.^{9–15} A detailed analysis of the ground-state absorption, the photoluminescence of donor–acceptor

^aKonarka Austria, Altenbergerstrasse 69, A-4040 Linz, Austria. E-mail: mscharber@konarka.com

^bKonarka Germany, Landgrabenstrasse 94, Nuremberg, Germany

^cJohannes Kepler University Linz, Altenbergerstrasse 69, A-4040 Linz, Austria

^dPhysics of Organic Semiconductors, Zernike Institute for Advanced Materials, University of Groningen, Nijenborgh 4, 9747 AG Groningen, The Netherlands. E-mail: M.A. Loi@rug.nl

† Electronic supplementary information (ESI) available. See DOI: 10.1039/c1ee02181h

Broader context

The development of new renewable energy technologies is most likely to be the most important challenge of mankind. The availability of cheap energy is mandatory for a positive development of societies and economic growth. Utilizing the energy from renewable sources will also help confining the effect of a global climate change. Solar energy resources are vast and available everywhere. However, with today's energy prices the economics of solar powered energy systems are often unfavorable. Organic solar cells offer a potential route to a low cost, large-scale photovoltaic technology which is based on earth-abundant materials and inexpensive production technologies. Despite recent advances in performance and lifetime, the understanding of the power conversion efficiency limiting factor is still incomplete. In this perspective, we consider key areas, the photoinduced charge generation process and the role of the organic semiconductor nano-morphology. A detailed understanding of both components will be essential for the further development of organic solar cells.

blends^{10,11} and also the electroluminescence¹⁵ of BHJ solar cells revealed that a long-lived, low energy transition occurs in various conjugated polymer–fullerene blends. The charge-transfer exciton (CTE) can be populated *via* direct excitation in the weak CT-band, *via* the photo-excitation of the donor or acceptor molecule followed by relaxation into the CTE-state or by the recombination of electrons and holes. After population, the CTE-state relaxes to the ground-state radiatively or non-radiatively or it may dissociate forming free charge carriers. The possibility of free charge carrier generation *via* sub-band-gap excitation has been demonstrated earlier¹⁶ applying a Fourier-transform infrared technique with very high sensitivity. As discussed by Deibel *et al.*¹⁷ it is still not fully understood which mechanism causes the dissociation of charge transfer excitons observed in various organic solar cells. The low dielectric constant of the organic semiconductors and the typical dimensions of CTEs suggest very high binding energies of the CTE and low dissociation yields. Mechanisms like interfacial dipoles, entropic effects,¹⁸ the excess energy from the charge transfer process and hot CT states, high local charge carrier mobilities,¹¹ polymer chain conformation¹⁹ and morphological effects²⁰ have been discussed. However, probably a combination of mechanisms leads to the efficient charge transfer exciton dissociation observed in BHJ cells.

The role of the CTE-state and its effect on the overall efficiency limit of bulk heterojunction devices are also still unclear. The energetic position of the CTE-state correlates with the open-circuit-voltage V_{oc} of BHJ cells,¹⁶ which suggests that the CTE-state is related to the lowest excited state in the system, consequently limiting the V_{oc} . Although in some cases rather weak, the CTE-emission may also be considered as an additional recombination loss of photo-excitations leading to lower photocurrents.¹⁴ On the other hand, a strong CT-absorption not subject to fast recombination could increase the number of generated free charge carriers and thus increase the power conversion efficiency of BHJ cells. According to the detailed balance concept^{4,21–23} a high electroluminescence quantum yield in solar cells is correlated with a high V_{oc} . In these terms, an increasing intensity of the CTE-emission, which is linked to the CT-absorption *via* the Einstein coefficient, could lead to solar cells with higher power conversion efficiencies.

Blends of poly[2,6-(4,4-bis-(2-ethylhexyl)-4H-cyclopenta[2,1-*b*:3,4-*b'*]-dithiophene)-*alt*-4,7-(2,1,3-benzothiadiazole)] (PCPDTBT) and [6,6]-phenyl-C₆₁-butyric acid methyl ester (PCBM)^{24,25} have recently shown interesting device performances in particular due to the absorption spectrum of the polymer in the near infrared spectral region. Photophysics^{26,27} and device physics²⁸ studies on the PCPDTBT–PCBM heterojunction identified a short lived bound electron–hole pair generated upon photo-excitation which limits the charge generation yield and causes an electric field dependent recombination loss in solar cells. Janssen *et al.* studied the effect of the processing additive diiodo-octane (DIO) on the photo-physics of PCPDTBT–PCBM blends and found that the formation of triplet states is reduced by adding DIO.²⁹

In the presented work the optical signature of charge transfer states in thin films and bulk-heterojunction solar cells made of PCPDTBT, blends of the polymer with [6,6]-phenyl-C₆₁-butyric acid methyl ester (PCBM) and the effect of octane-dithiol (ODT) as processing additive are investigated. The effect of ODT on the

electrical and optical properties of PCPDTBT:PCBM blends was studied earlier. Cho *et al.*³⁰ reported that ODT leads to an enhancement of the mobility of electrons and holes in an organic field effect transistor (OFET). In addition, they found that the additives remaining in the film strongly reduce the hole mobility and that a careful drying procedure is necessary to reach good OFET performances. The effect of ODT on the morphology was studied by atomic force microscopy and transmission electron microscopy.^{31,32} Fibril structures surrounded by fullerene rich regions were found in films processed with ODT. In more recent papers, an increase of the donor and acceptor domain size from ~5 nm to ~8 nm was reported for thin films processed with additives³³ and also GIWAXS (Grazing Incidence Wide Angle X-ray Scattering) data proved that the polymorph correlation lengths of PCPDTBT domains increase upon the use of ODT.³⁴

The Heeger group also studied the effect of ODT on the excitation dynamics in thin PCPDTBT–PCBM films.^{26,35} They found that the ODT increases the generation of free charge carriers similar to a thermal annealing of a poly-3-hexyl-thiophene:PCBM blend but the effect was found to be not strong enough to explain the observed increase in the power conversion efficiency of BHJ-devices processed using ODT. Hwang *et al.*²⁶ conclude that the higher charge carrier mobility is the main source for the higher device efficiencies.

In the work presented here, a strong CTE-emission in PCPDTBT–PCBM blend films is found when chlorobenzene is used as the processing solvent. Upon adding ODT, the CTE-emission is reduced significantly. Following the recipe developed by the Heeger group²⁵ we prepared PCPDTBT–PCBM BHJ-cells with and without processing additive and observed the ODT-effect reported earlier on the power conversion efficiency. Photoluminescence and electroluminescence studies performed on functional solar cells show the same trend; the use of ODT as processing additive does quench the CTE-emission substantially. The presented results suggest that the formation of a charge transfer state is a loss process in PCPDTBT–PCBM devices which can be reduced by a processing additive such as ODT.

Experimental

For photoluminescence measurements, thin films were blade-coated on cleaned microscope slides. Samples were excited by a 150 fs pulsed Kerr mode locked Ti-sapphire laser at 760 nm or frequency doubled at 380 nm. The steady state photoluminescence emission was measured with an Andor iDus InGaAs array detector. The spectra are corrected for the spectral response of the setup. Typical excitation power densities were ~1 mW on a focused laser spot of about 100 μm of diameter. The time-resolved PL was recorded by a near infrared sensitive Hamamatsu streak camera working in synchro-scan mode. All the measurements were performed at room temperature. To avoid degradation, all samples were edge-sealed with a glass slide and a UV-curable epoxy in a N₂-filled glovebox before the measurements.

Diodes and BHJ devices were prepared as described earlier.²⁴ Chlorobenzene was used as processing solvent and an octane-dithiol (ODT) concentration of 30 μg per ml solvent was selected following the procedure described in ref. 25. For blend devices the weight ratio of PCPDTBT and PCBM was 1 : 2. Solar cells

were characterized on an ORIEL solar simulator. External Quantum Efficiencies (EQEs) were measured by using a lock-in amplifier (SR830, Stanford Research Systems) with a current preamplifier (HMS-74) under short circuit conditions. The devices were illuminated by monochromatic light from a xenon lamp passing through a monochromator (Oriel Cornerstone) with a typical intensity of a few μW , between the Xenon lamp and the monochromator a mechanical chopper was mounted. Typical chopping frequencies in the range of 10–200 Hz were used. A calibrated silicon diode (Hamamatsu S2281) is used as a reference. Photoluminescence and electroluminescence spectra of various devices were measured using a Shamrock SR-303i monochromator and an Andor iDus Si-CCD. Devices and diodes were excited at 655 nm using a solid-state laser. The light intensity was chosen such that the devices delivered short circuit currents comparable to an AM1.5G illumination. A set of long-pass filters was used to avoid any distortion of the recorded spectra by the laser light. Spectra recorded with the CCD-camera were corrected for the spectral response of the experimental setup.

Despite the careful corrects, spectra recorded with the near IR InGaAs detector array camera show slightly different intensity distributions *versus* the wavelength. We relate this to the different samples used in the experiments. While some measurements including the transient PL were done on thin films deposited on glass substrates other measurements were done on completed BHJ solar cells. The conductive electrodes cause an enhanced interference effect and especially the ITO and PEDOT:PSS layer leads to additional absorption losses in the near IR range overall alternating the emission spectra of the studied devices.

Results and discussion

In Fig. 1(a) the photoluminescence spectra of thin films made of pristine PCPDTBT and blends of PCPDTBT and PCBM mixed at weight ratios of 1 : 0.5, 1 : 1 and 1 : 2 are compared. The pristine polymer film shows a broad emission with a maximum around 830 nm and a shoulder around 920 nm. Upon addition of PCBM, the overall photoluminescence intensity is reduced due to

the exciton dissociation by the fullerene acceptor and a second emission band with a maximum around 1000 nm appears.

The emitting species in the pristine polymer is relatively short lived with a photoluminescence lifetime of ~ 200 ps (Fig. 1(b)). Adding PCBM to the polymer leads to a faster decay of the high energy photoluminescence (800–830 nm) with a fast component of roughly 10 ps and a remaining longer tail of 350 ps. In Fig. 1 (b) also the photoluminescence decays of the pristine polymer and of the polymer–fullerene blend recorded between 950 and 1050 nm are shown. While the pristine polymer exhibits the same dynamics at all emission frequencies, different decay times are found for the blend. The decay of the low energy feature of the polymer–fullerene BHJ can be fitted with a bi-exponential function of time constants $\tau_1 \approx 40$ ps and $\tau_2 \approx 780$ ps.

Such a long lifetime and the spectral position suggest the formation of new excited species in the blend which we assign to a charge transfer exciton (CTE).

Fig. 2(a) shows the photoluminescence spectra of a PCPDTBT film and PCPDTBT : PCBM (weight ratio 1 : 1) films processed with and without octane-dithiol. The film processed with ODT shows a reduced low energy emission as shown in Fig. 2(a) and also a much shorter decay time. While the PL decay in the range of 950–1050 nm of the PCPDTBT:PCBM thin film has a dominant component of ~ 660 ps, the film processed with ODT has a fast component of 25 ps and a remaining tail of ~ 210 ps. This shows that the formation of long-lived species is strongly suppressed in films processed using ODT and that the PL is dominated by the polymeric component. It is important to note that due to the spectral overlap of the polymeric and the CTE emission a precise determination of the lifetimes of the two species is very difficult. Extracting the PL-decay curves in different parts of the spectra leads to slight lifetime variations.

In Fig. 3(a) current–voltage curves measured under illumination of a device prepared from chlorobenzene (CB) and a device prepared from a mixture of chlorobenzene and ODT are shown. Devices processed with additive show a higher short circuit current and also higher electrical fill factors but a lower open circuit voltage. In Fig. 3(b) the External Quantum Efficiencies (EQEs) of various devices are shown. Compared to the pristine components (PCPDTBT, PCBM) the EQE spectra of the

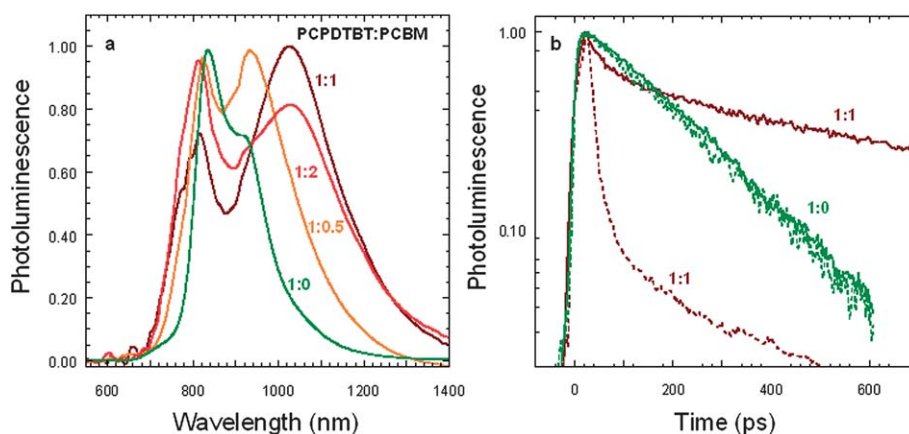


Fig. 1 (a) Normalized photoluminescence spectra of the pristine PCPDTBT thin film and of the polymer:PCBM BHJ in different weight ratios. (b) Time resolved photoluminescence of the pristine polymer and of the 1 : 0.5 BHJ measured at 800–830 nm (dotted line) and at 950–1050 nm (full line).

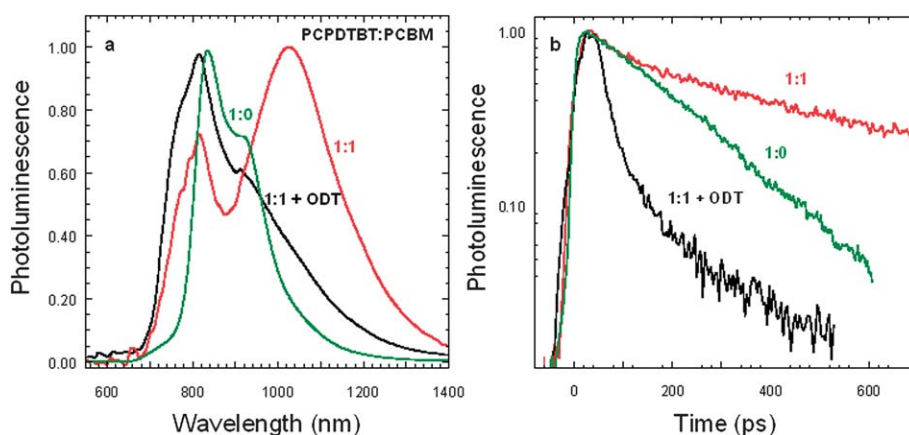


Fig. 2 (a) Normalized photoluminescence spectra of the pristine polymer thin film and of the 1 : 1 BJJ with and without ODT. (b) Photoluminescence decays of the pristine polymer and of the BJJ 1 : 1 with and without ODT, measured in the spectral range between 950 nm and 1050 nm.

bulk-heterojunction devices show a shoulder extending significantly further to the infra-red. Such a red-shift of the EQE upon the addition of PCBM has been observed in various different BJJ-solar cells and has been assigned to the ground-state absorption of a charge transfer complex formed between the donor polymer and PCBM.^{16,23} The experimental results summarized in Fig. 3(b) propose that a weak CTE-absorption is present in both types of BJJ solar cells.

In Fig. 4(a) the photoluminescence spectra of PCPDTBT-based diodes processed with and without ODT are compared. The use of the processing additive leads to a negligible shift of the emission maximum for the pristine polymer.

In Fig. 4(b) the bias-dependence of the photoluminescence of a PCPDTBT/PCBM bulk-heterojunction solar cell processed with ODT is shown. The recorded emission spectra show a maximum around 820 nm and a low energy shoulder at about 900 nm. The solar cell shows a more pronounced low energy feature compared to the polymer only device. Varying the applied bias from -1 V to $+1.4$ V the shape of the emission spectrum does not change. In addition, only small variations in

the overall amplitude are observed. The maximum intensity can be achieved by applying a voltage corresponding to the open circuit voltage of the device. By applying more negative voltages the amplitude spectrum is reduced further. At -5 V a PL intensity reduction of $\sim 3\%$ could be achieved. In Fig. 4(c) and (d) the bias-dependences ((c) forward and (d) reverse) of the photoluminescence of a PCPDTBT/PCBM bulk-heterojunction solar cell processed without ODT are shown. The spectrum at zero bias comprises a broad emission with a shoulder around 850 nm and an increasing signal between 900 and 1000 nm. Due to the limited spectral sensitivity of the applied detector, the maximum of the CTE emission cannot be resolved in these experiments. Upon applying a forward bias the intensity of the low energy feature increases while applying a reverse bias, the same feature loses intensity. A similar dependence of the photoluminescence intensity of polymer–fullerene blends on an electric field has been observed earlier^{36,37} and together with the time-resolved photoluminescence measurements shown in Fig. 2 allows assignment of the bias-dependent emission to the radiative recombination of the charge transfer exciton. In Fig. 5(a)

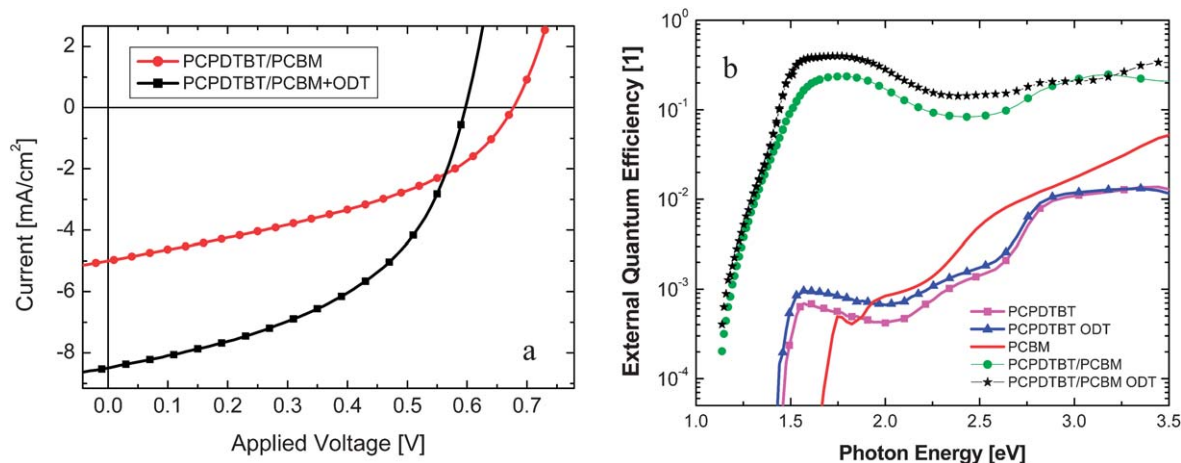


Fig. 3 (a) Current–voltage characteristics of PCPDTBT–PCBM bulk-heterojunction solar cells processed with (squares) and without (circles) additive. (b) External Quantum Efficiency spectra of a PCPDTBT diode (squares), PCPDTBT diode processed with ODT (triangles), PCBM-diode (line), PCPDTBT–PCBM bulk-heterojunction solar cell without (circles) and with (stars) octane-dithiol.

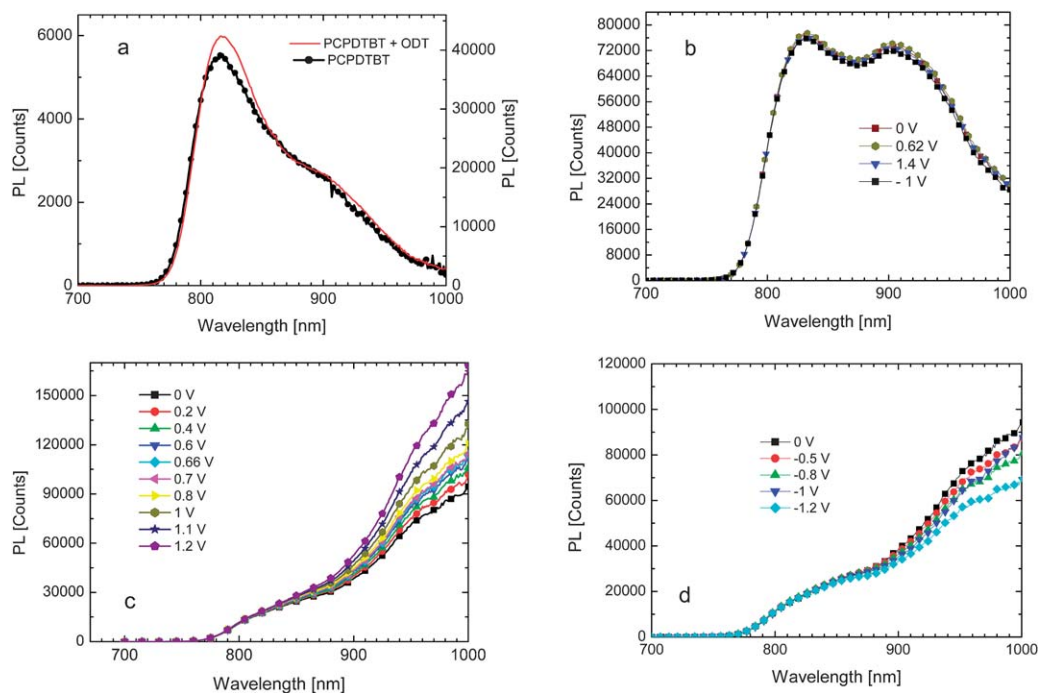


Fig. 4 (a) Photoluminescence measured on PCPDTBT-diodes processed with and without ODT. (b) Bias-dependence (forward and reverse) of PL of a BJJ-solar cell processed with ODT. (c) Bias-dependence (forward) of PL of a BJJ-solar cell processed without ODT. (d) Bias-dependence (reverse) of PL of a BJJ-solar cell processed without ODT.

electroluminescence spectra of a PCPDTBT:PCBM solar cell processed *without* ODT, recorded at different forward biases, are shown. A broad feature with a maximum outside the sensitivity range of the detector is observed which increases upon increasing the bias. In the ESI† the electroluminescence spectra of different devices recorded with an infrared sensitive detector (InGaAs) are shown. The electroluminescence signal peaks around 1100 nm in good agreement with the photoluminescence measurements shown in Fig. 1.

In Fig. 5(b) the electroluminescence spectra at different biases of the solar cell processed with the additive ODT are summarized. The signals are very weak and the shape of the observed spectra is similar to the corresponding photoluminescence spectra with a more pronounced low energy shoulder.

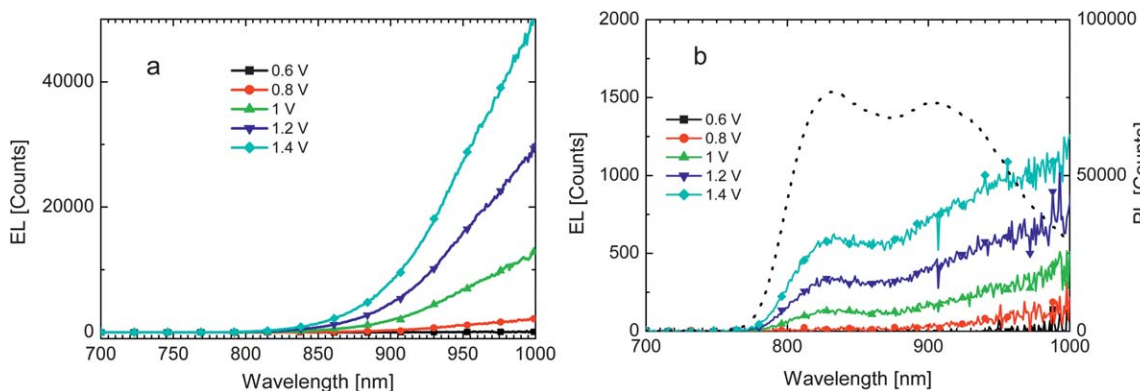


Fig. 5 Electroluminescence of PCPDTBT/PCBM devices processed without ODT (a) and with ODT (b). For comparison the photoluminescence spectrum of the same device at zero bias is added to (b) (dotted line).

and is also seen as a long lived component in the transient PL measurements. In this case the CTE-emission does not show a significant electric field dependence.

Considering all presented experimental results and the work reported on the morphological effects of processing additives,^{31–33} the arrangement of the donor and acceptor molecules on a nanometre scale appears to be essential for an efficient CTE dissociation.²⁰ A qualitative description presented by Tvingstedt *et al.*³⁷ may be used to explain the experimental findings described above. When PCPDTBT:PCBM blend films are prepared without additive, the donor and the acceptor are mixed on a molecular level. This leads to strong spatial and electronic disorder and predominantly localized excitations and charge carriers are generated. The disorder may also lead to more intimate charge transfer excitons resulting in larger binding energies of the CTE-states. In a bulk-heterojunction solar cell the internal electric field can only dissociate a fraction of the photo-generated CTE-states and a substantial part of the CT-excitons are lost under typical operation conditions.

In contrast, blends processed with additive show a more ordered nano-morphology with several nanometre sized domains of pristine donor and acceptor materials. Charge transfer excitons generated at the interface between donor and acceptor domains can delocalize over a larger volume which decreases their binding energy. Under operation conditions a dominant part of the CT-excitons (see Fig. 3(b)) are converted into charge carriers leading to larger photocurrents and higher efficiencies. The residual CT-emission results from volume fractions with lower molecular ordering. By optimizing the processing conditions one may be able to minimize CT-emission intensity further. An alternative explanation for the reduction of the low energy emission by ODT may be related to the fact that small amounts of surfactant are still present in the solid film even after extensive drying. Solid-state NMR studies³⁸ revealed that ODT acts as a plasticizer inducing an additional ordering of the polymer chains. To work as a plasticizer the ODT molecules need to intercalate into the polymer domains and could also act as a spacer between the donor and acceptor molecules. This would increase the average distance between donors and acceptors reducing the probability that a CTE is formed. To work as a spacer or plasticizer the dimensions of the used additive should play an important role. Tests with different dithiols (hexane, octane and nonane) show that the use of hexane-dithiol and nonane-dithiol results in lower device efficiencies compared to octane-dithiol supporting this idea.³⁹

In the investigated polymer–fullerene blend the appearance of the pronounced CTE emission is accompanied by a low external quantum efficiency and electrical fill factor, leading to a low overall power-conversion efficiency. In contrast, the reduction of the CTE-emission by fine-tuning the morphology of the photo-active layer results in higher external quantum efficiencies and power conversion efficiencies, despite the fact that the open circuit voltage of devices processed with additive is slightly lower. The origin of the reduced V_{oc} is not fully understood. Higher charge carrier mobilities induced by octane-dithiol may cause a faster charge carrier recombination leading to a lower steady-state charge carrier concentration under open-circuit conditions. This is supported by transient photovoltage measurements showing slightly shorter charge carrier lifetimes for solar cells

with additive.⁴⁰ The morphological changes induced by the additive may also modify the distribution of the density of states in the semiconductor layer which could result in faster recombination kinetics leading to low V_{oc} .⁴¹

A similar relation between the CTE-emission intensity and the short circuit current was also found for BHJ cells based on MDMO-PPV and different fullerene derivatives.¹⁴ This observation is not fully in line with the detailed balance principle which has been applied to bulk-heterojunction solar cells recently.^{21–23} The detailed balance predicts that a high charge generation quantum yield (EQE) is achieved when the photo-active absorber layer shows a high electroluminescence/photo-luminescence quantum yield. PCPDTBT–PCBM blends do show the opposite trend indicating the necessity of further investigations. We believe that a significant population of an emissive charge transfer exciton will always lead to a field dependent charge generation and will limit the number of extracted charge carriers in bulk-heterojunction solar cells, especially when the cells are operated at lower internal fields around the maximum power point.

In summary, we have studied the effect of octane-dithiol on the optical properties of thin film blends of poly[2,6-(4,4-bis-(2-ethylhexyl)-4*H*-cyclopenta[2,1-*b*;3,4-*b'*]-dithiophene)-*alt*-4,7-(2,1,3-benzothiadiazole)] and [6,6]-phenyl- C_{61} -butyric acid methyl ester. Films processed without octane-dithiol show a long-lived, red-shifted, emission which we assign to a charge transfer state emission. The intensity of this emission correlates with the percentage of fullerene derivatives in the blend confirming the interfacial nature of the CTE state. The use of octane-dithiol strongly suppresses the CTE formation and emission. We propose that the quenching of the CTE-emission is related to a morphological effect. The presented work emphasises again the importance of the arrangement of donor and acceptor components in organic solar cells. Besides an optimization of the optical and electrical properties of the individual components also the morphology of the absorber layer needs to be controlled for achieving high charge generation efficiencies.

Acknowledgements

M.B., G.M. and T.F. would like to thank the FFG (Die Österreichische Forschungsförderungsgesellschaft) for financial support (grant number 818046).

References

- G. Dennler, M. C. Scharber and C. J. Brabec, *Adv. Mater.*, 2009, **21**, 1323.
- L. A. Green, K. Emery, Y. Hishikawa and W. Warta, *Prog. Photovoltaics*, 2011, **19**, 565.
- M. C. Scharber, D. Mühlbacher, M. Koppe, P. Denk, C. Waldauf, A. J. Heeger and C. J. Brabec, *Adv. Mater.*, 2006, **18**, 789.
- W. Shockley and H. J. Queisser, *J. Appl. Phys.*, 1961, **32**, 510.
- X. Yang and J. Loos, *Macromolecules*, 2007, **40**, 1353.
- A. Pivrikas, N. S. Sariciftci, G. Juska and R. Österbacka, *Prog. Photovolt.: Res. Appl.*, 2007, **15**, 677.
- L. J. A. Koster, V. D. Mihailetschi, M. Lenes and P. W. M. Blom, *Organic Photovoltaics: Materials, Device Physics, and Manufacturing Technologies*, ed. C. Brabec, V. Dyakonov and U. Scherf, Wiley-VCH Verlag GmbH & Co, KGaA, Weinheim, 2008, ch. 10.
- D. Veldman, S. C. J. Meskers and R. A. J. Janssen, *Adv. Funct. Mater.*, 2009, **19**, 1939.

- 9 J. J. Benson-Smith, L. Goris, K. Vandewal, K. Haenen, J. V. Manca, D. Vanderzande, D. D. C. Bradley and J. Nelson, *Adv. Funct. Mater.*, 2007, **17**, 451.
- 10 M. A. Loi, S. Toffanin, M. Muccini, M. Forster, U. Scherf and M. Scharber, *Adv. Funct. Mater.*, 2007, **17**, 2111.
- 11 D. Veldman, Ö. Ipek, S. C. J. Meskers, J. Sweelssen, M. M. Koetse, S. C. Veenstra, J. M. Kroon, S. S. van Bavel, J. Loos and R. A. J. Janssen, *J. Am. Chem. Soc.*, 2008, **130**, 7721.
- 12 D. Veldman, S. C. J. Meskers and R. A. J. Janssen, *Adv. Funct. Mater.*, 2009, **19**, 1939.
- 13 T. Drori, C.-X. Sheng, A. Ndobé, S. Singh, J. Holt and Z. V. Vardeny, *Phys. Rev. Lett.*, 2008, **101**, 037401.
- 14 M. Hallermann, S. Haneder, E. Da Como, J. Feldmann, M. Izquierdo, S. Filippone, N. Martín, S. Jüchter and E. von Hauff, *Appl. Phys. Lett.*, 2008, **93**, 053307.
- 15 K. Tvingstedt, K. Vandewal, A. Gadisa, F. Zhang, J. Manca and O. Inganäs, *J. Am. Chem. Soc.*, 2009, **131**, 11819.
- 16 K. Vandewal, A. Gadisa, W. D. Oosterbaan, S. Bertho, F. Banishoeib, I. Van Severen, L. Lutsen, T. J. Cleij, D. Vanderzande and J. V. Manca, *Adv. Funct. Mater.*, 2008, **18**, 2064.
- 17 C. Deibel, T. Strobel and V. Dyakonov, *Adv. Mater.*, 2010, **22**, 4097.
- 18 T. R. Clarke and J. R. Durrant, *Chem. Rev.*, 2010, **110**, 6736.
- 19 M. Hallermann, I. Kriegel, E. Da Como, J. Berger, E. von Hauff and J. Feldmann, *Adv. Funct. Mater.*, 2009, **19**, 3662.
- 20 M. C. Scharber, M. Koppe, J. Gao, F. Cordella, M. A. Loi, P. Denk, M. Morana, H.-J. Egelhaaf, K. Forberich, G. Dennler, R. Gaudiana, D. Waller, Z. Zhu, X. Shi and C. J. Brabec, *Adv. Mater.*, 2010, **22**, 367.
- 21 T. Kirchartz, K. Taretto and U. Rau, *J. Phys. Chem. C*, 2009, **113**, 17958.
- 22 T. Kirchartz, J. Mattheis and U. Rau, *Phys. Rev. B: Condens. Matter Mater. Phys.*, 2008, **78**, 235320.
- 23 K. Vandewal, K. Tvingstedt, A. Gadisa, O. Inganäs and J. V. Manca, *Nat. Mater.*, 2009, **8**, 904.
- 24 D. Mühlbacher, M. Scharber, M. Morana, Z. Zhu, D. Waller, R. Gaudiana and C. Brabec, *Adv. Mater.*, 2006, **18**, 2884.
- 25 J. Peet, J. Y. Kim, N. E. Coates, W. L. Ma, D. Moses, A. J. Heeger and G. C. Bazan, *Nat. Mater.*, 2007, **6**, 497.
- 26 I.-W. Hwang, S. Cho, J. Y. Kim, K. Lee, N. E. Coates, D. Moses and A. J. Heeger, *J. Appl. Phys.*, 2008, **104**, 033706.
- 27 D. Jarzab, F. Cordella, J. Gao, M. Scharber, H.-J. Egelhaaf and M. A. Loi, *Adv. Energy Mater.*, 2011, **1**, 604.
- 28 M. Lenes, M. Morana, C. J. Brabec and P. W. M. Blom, *Adv. Funct. Mater.*, 2009, **19**, 1106.
- 29 D. Di Nuzzo, A. Aguirre, M. Shahid, V. S. Gevaerts, S. C. J. Meskers and R. A. J. Janssen, *Adv. Mater.*, 2010, **22**, 4321.
- 30 S. Cho, J. K. Lee, J. S. Moon, J. Yue, K. Lee and A. J. Heeger, *Org. Electron.*, 2008, **9**, 1107.
- 31 J. K. Lee, W. L. Ma, C. J. Brabec, J. Yuen, J. S. Moon, J. Y. Kim, K. Lee, G. C. Bazan and A. J. Heeger, *J. Am. Chem. Soc.*, 2008, **130**, 3619.
- 32 M. Morana, H. Azimi, G. Dennler, H.-J. Egelhaaf, M. Scharber, K. Forberich, J. Hauch, R. Gaudiana, D. Waller, Z. Zhu, K. Hingerl, S. S. van Bavel, J. Loos and C. J. Brabec, *Adv. Funct. Mater.*, 2010, **20**, 1180.
- 33 M. Dante, A. Garcia and T.-Q. Nguyen, *J. Phys. Chem. C*, 2009, **113**, 1596.
- 34 U. T. Rogers, K. Schmidt, M. F. Toney, E. J. Kramer and G. C. Bazan, *Adv. Mater.*, 2011, **23**, 2284.
- 35 C. Soci, I.-W. Hwang, D. Moses, Z. Zhu, D. Waller, R. Gaudiana, C. J. Brabec and A. J. Heeger, *Adv. Funct. Mater.*, 2007, **17**, 632.
- 36 Y. Zhou, K. Tvingstedt, F. Zhang, C. Du, W.-X. Ni, M. R. Andersson and O. Inganäs, *Adv. Funct. Mater.*, 2009, **19**, 3293.
- 37 K. Tvingstedt, K. Vandewal, F. Zhang and O. Inganäs, *J. Phys. Chem. C*, 2010, **114**, 21824.
- 38 S. Chambon, R. Mens, K. Vandewal, E. Clodic, M. Scharber, L. Lutsen, J. Gelmann, J. Manca, D. Vanderzande and P. Adriaenssens, *Sol. Energy Mater. Sol. Cells*, accepted.
- 39 Unpublished.
- 40 T. Agostinelli, T. A. M. Ferenczi, E. Pires, S. Foster, A. Maurano, C. Müller, A. Ballantyne, M. Hampton, S. Lilliu, M. Campoy-Quiles, H. Azimi, M. Morana, D. D. C. Bradley, J. Durrant, J. E. Macdonald, N. Stingelin and J. Nelson, *J. Polym. Sci., Part B: Polym. Phys.*, 2011, **49**, 717.
- 41 G. Garcia-Belmonte, P. P. Boix, J. Bisquert, M. Lenes, H. J. Bolink, A. La Rosa, S. Filippone and N. Martín, *J. Phys. Chem. Lett.*, 2010, **1**, 2566–2571.